

DEGRADATION OF EMERGING AND PERSISTENT POLLUTANTS: SYNERGISTIC SUNLIGHT PHOTOCATALYTIC ACTIVITY OF CoS/ZnO/XC

Paula M. R. M. Santos¹, Ikaro Tessaro¹, Luiza F. Pinheiro¹, Flavio H. C. Boldrin¹, Laila G. Andrade¹, Cesar A. F. M. P. Lico¹, Lucas H. Cardia¹, Bruno H. B. Silva¹, Nicolas P. Moraes² & Liana A. Rodrigues^{1*}

¹ Escola de Engenharia de Lorena-EEL/USP, Estrada Municipal do Campinho S/N, CEP 12602-810, Lorena, São Paulo, Brazil.

² São Carlos Institute of Chemistry, University of São Paulo, Av. Trab. São Carlense, 400 - Parque Arnold Schimidt, São Carlos - SP, 13566-59

* Corresponding author's email address: liana.r@usp.br

ABSTRACT

In recent years, growing environmental pollution awareness has led to intensive research on clean technologies to mitigate pollution effects. Advances in the pharmaceutical industry have resulted in inappropriate disposal of various products, necessitating effective treatment methods. In the context of environmental biotechnology, the process of detecting and degrading emerging micropollutants associated with advanced oxidative processes has been proving promising and necessary. Heterogeneous photocatalysis, a green and sustainable technology, has gained interest due to addressing pollution using sunlight energy. Research aims to develop semiconductors with lower bandgaps, higher stability, and non-toxicity. This study focused on the photocatalytic degradation of salicylic acid (SA), a recalcitrant molecule widely used in dermatology and medicine. Characterization of synthesized materials through X-ray diffraction (XRD) and scanning electron microscopy (SEM) provided insights into their structure and elemental distribution. The study included materials such as 5% CoS/ZnO/0.250 XC at 600°C, ZnO/0.250 XC at 600°C, ZnO at 600°C, and CoS at 750°C. The presence of Carbon Xerogel (XC) significantly improved photocatalytic performance, enhancing charge transfer efficiency and catalytic properties. These findings highlight the potential of these materials for practical environmental applications.

Keywords: Heterogeneous photocatalysis. Photocatalytic degradation. Salicylic acid. Carbon xerogel. X-ray diffraction.

1 INTRODUCTION

In recent years, growing awareness about environmental pollution has stimulated intensive research in order to develop clean technologies capable of minimizing pollution effects¹. With advancements in the pharmaceutical industry, an increasing number of products are being generated without proper disposal care, such as pharmaceuticals, steroids, soaps, and sunscreens².

In the field of environmental biotechnology, there is a growing recognition of the importance of advanced methods to detect and degrade emerging micropollutants. The use of advanced oxidative processes has emerged as a promising approach to address challenges associated with environmental pollution². These methods not only offer efficiency in the removal and degradation of persistent substances but also promote more effective waste treatment practices aligned with principles of environmental conservation and public safety¹⁻². Heterogeneous photocatalysis, as a green and sustainable technology, has attracted considerable interest in addressing this problem using sunlight energy³. Research in photocatalysis is increasingly focused on creating semiconductors with a lower bandgap, higher chemical stability, resistance to photocorrosion, low cost, and non-toxicity to the environment⁴. The degradation of salicylic acid (SA), a recalcitrant molecule frequently employed for treating infectious diseases in humans and animals, has been widely investigated due to its extensive use in dermatological, cosmetic, food, and medicinal formulations⁵.

CoS is a p-type semiconductor that can be used as a cocatalyst, contributing to accelerating the separation of photogenerated charges and increasing the speed of reactions that occur during the photocatalytic process due to its large number of active sites available for the reaction and high conductivity electricity that improves the mass transfer rate across the catalyst surface, resulting in a significant increase in the efficiency of the piezo-photocatalyst^{6,7}.

2 MATERIAL & METHODS

The synthesis of the CoS unary material, tested and analyzed for obtaining cobalt sulfide (CoS). The reagents used included thioacetamide (C_2H_5NS , M.W. 75.13) and hexahydrated cobalt nitrate ($Co(NO_3)_2 \cdot 6H_2O$, CAS [10026-22-9]). Initially, for the preparation of the primary CoS material, synthesis routes were explored using a heating plate coupled with a reflux system. In this process, 2.5 g of cobalt nitrate were dissolved in 100 mL of distilled water until reaching a temperature of 150°C. Subsequently, thioacetamide was dissolved as a reagent in stoichiometric concentrations. The mixture was maintained at 150°C for 3 hours under constant magnetic stirring. Finally, the precipitates resulting from the syntheses were subjected to repeated washings with deionized water until reaching a neutral pH. Then, the material was dried in an oven at (100°C, 72h), ground, and then sieved through an analytical sieve mesh 325 and calcined at a temperature of 750°C for 30 minutes.

To obtain the ternary compound 5% CoS/ZnO/XC, consisting of carbon xerogel, zinc oxide, and cobalt sulfide, the subsequent procedure was followed: a mass of 8.098 g of $ZnCl_2$ (zinc chloride) was dissolved in 20 mL of deionized water, along with 0.255 g of calcined cobalt sulfide, in 30 mL of deionized water, while 0.25 g of tannin was added and dissolved in 50 mL of deionized water containing 7.19 g of KOH. Subsequently, the precipitates resulting from the syntheses were subjected to repeated washings

with deionized water until a neutral pH was reached. The material was then dried in an oven at 100°C for 72 hours, ground, and sieved through a 325-mesh analytical sieve. Finally, the compounds were calcined at 600°C for 30 minutes.

The utilized semiconductors underwent characterization using X-ray diffraction (XRD) to understand the atomic distribution, identify crystalline phases, and determine crystallographic parameters. The morphology and elemental composition of the samples were assessed through scanning electron microscopy (SEM) and Energy-dispersive X-ray spectroscopy (EDS), respectively.

Tests to assess the photocatalytic activity of the materials were conducted in a 0.5 L reactor, with constant magnetic stirring and temperature controlled at 25°C. Each test involved adding 0.1 g of the evaluated photocatalyst and 0.5 L of a solution of salicylic acid (SA) at 10 mg L⁻¹ to the reactor, kept in the dark to achieve adsorption-desorption equilibrium between SA and the catalyst. After equilibrium was reached, the samples were exposed to irradiation from a 300 W lamp to simulate sunlight radiation. The concentration of SA was measured with a UV-Vis spectrophotometer at 296 nm after filtering the samples. Samples were collected at 15-minute intervals initially, followed by 30-minute intervals, over a period of 300 minutes or until complete degradation of the pollutant.

3 RESULTS & DISCUSSION

The results presented in the semiconductor characterizations were followed by photocatalytic degradation tests, aiming at the elimination of emerging pollutants. These materials were previously analyzed regarding their structure and composition before being assessed for their effectiveness in degradation these contaminants.

X-ray diffraction (XRD) analysis provided information about the structure and crystallinity of the unary materials presented in the diffractogram shown in Figure 1, demonstrating the identification of peaks and bands of interest present in the synthesized materials in relation to the ICDD codes referenced in the literature, available in the High Score Plus database.

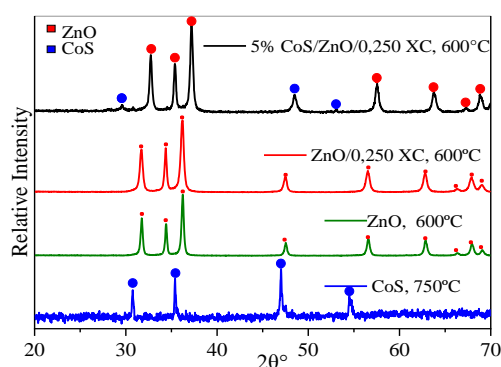


Figure 1 X-ray diffraction (XRD) patterns obtained for the materials synthesized in this study.

The diffractograms presented in Figure 1 correspond to four different synthesized samples: 5% CoS/ZnO/0.250 XC at 600°C, ZnO/0.250 XC at 600°C, ZnO at 600°C, and CoS at 750°C. Each diffractogram reveals the characteristic peaks of X-ray diffraction for the materials present in each sample.

In the diffractogram of the first material, 5% CoS/ZnO/0.250 XC at 600°C, characteristic peaks for both CoS and ZnO are observed, indicating the presence of both materials. The peaks of CoS are consistent with ICDD 00-001-1279, while those of ZnO correspond to ICDD 03-065-3418. This suggests that this sample is a mixture of CoS and ZnO⁹. The diffractograms of the second and third materials, ZnO/0.250 XC at 600°C and ZnO at 600°C, respectively, show only characteristic peaks of ZnO. This indicates that these samples are mainly composed of ZnO, without the detectable presence of other materials. Finally, in the diffractogram of the fourth material, CoS at 750°C, characteristic peaks of CoS are observed, according to ICDD 01-075-0576. This indicates that this sample is predominantly composed of CoS⁹. These results are consistent with the analysis of X-ray diffraction patterns, allowing the identification of the crystalline phases present in each sample. The correlation of experimental data with theoretical patterns from ICDD suggests good agreement, validating the composition and crystalline structure of the synthesized materials.

The Figure 2 presents micrographs obtained by scanning electron microscopy (SEM) along with Energy Dispersive Spectroscopy (EDS) data for the material under analysis. Considering the crystallite sizes determined earlier, 42.44 for the ternary material ZnO/0.250 XC, 600°C and 66.76 for ZnO, 600°C, this analysis will provide a detailed view of the surface morphology and elemental distribution of the material.

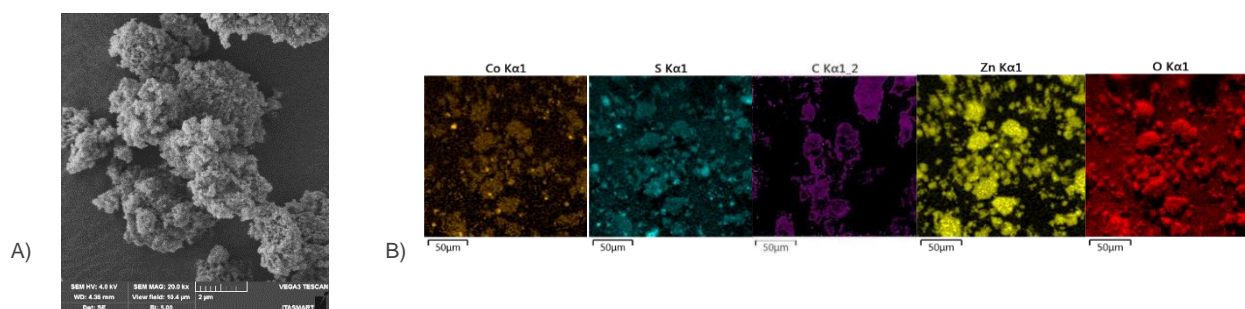


Figure 2 Displays A) scanning electron microscopy and B) elemental distribution analysis of the material, of ternary material.

The results from the micrographs and EDS mapping indicate that all materials exhibit a homogeneous distribution of their constituent elements. This homogeneity is crucial for enhancing charge transfer efficiency at the heterojunctions formed between the different components of the composites. The rapid charge transfer at the material interface contributes to reducing the recombination of photo-generated charges, resulting in higher efficiency in photocatalytic applications. Additionally, the incorporation of CoS and carbon xerogel into ZnO shows promising potential in improving catalytic properties due to the formation of new active sites and enhancement in electronic conduction. These prepared materials demonstrate that the doping strategy and composite formation can be effective for the synthesis of advanced photocatalysts, with potential for various environmental and energy applications¹⁰.

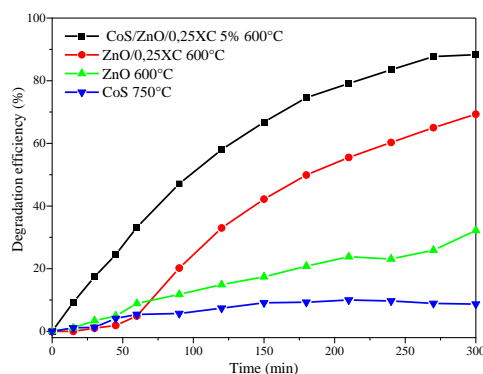


Figure 3 Results of photocatalytic tests for the degradation of SA.

The results from photocatalytic tests for the degradation of SA, as depicted in Figure 3, highlight the influence of Carbon Xerogel (XC) presence on photocatalytic performance, as revealed by synthesis studies. The structural stability indicated in the diffraction patterns suggests improvements in catalytic properties, contributing to enhanced results in degradation tests under sunlight irradiation. The effectiveness of the CoS and ZnO combination, as evidenced in the diffraction patterns, further underscores the efficiency of these materials in pollutant degradation¹¹. The consistency between the diffraction patterns and degradation test results suggests that the careful selection of materials, including the presence of Carbon Xerogel, can significantly optimize the catalytic efficiency of the photocatalyst in pollutant degradation processes under sunlight irradiation. This integrated approach between structural analysis and catalytic performance provides a solid foundation for future practical applications of these materials in heterogeneous photocatalysis processes¹².

4 CONCLUSION

The photocatalytic degradation tests confirmed the effectiveness of the synthesized materials in degradation emerging pollutants. The inclusion of Carbon Xerogel (XC) significantly enhanced photocatalytic performance. X-ray diffraction (XRD) and electron microscopy analyses revealed a homogeneous distribution of elements and favorable surface morphology for efficient charge transfer. The structural stability and improved catalytic properties of the CoS and ZnO combination, as indicated by diffraction patterns, underscore the efficiency of these materials in pollutant degradation. These findings highlight the potential of these advanced photocatalysts for practical applications in environmental pollutant degradation through heterogeneous photocatalysis.

REFERENCES

- GAO, J., WU, D., XIAO, Q., RANDHAWA, A., LIU, Q., & ZHANG, T. (2023). *Environmental Science and Pollution Research*, 30(11), 31954-31976.
- RATCHNASHREE, S. R., KARMEGAM, N., SELVAM, M., MANIKANDAN, S., DEENA, S. R., SUBBAIYA, R., & GOVARTHANAN, M. (2023). *Science of The Total Environment*, 166563.
- GOODARZI, N., ASHRAFI-PEYMAN, Z., KHANI, E., & MOSHFEGH, A. Z. (2023). *Catalysts*, 13(7), 1102.
- CARMINATI, S. A., RODRÍGUEZ-GUTIÉRREZ, I., DE MORAIS, A., DA SILVA, B. L., MELO, M. A., SOUZA, F. L., & NOGUEIRA, A. F. (2021). *RSC advances*, 11(24), 14374-14398.
- MOHSIN, N., HERNANDEZ, L. E., MARTIN, M. R., DOES, A. V., & NOURI, K. (2022). *Dermatologic therapy*, 35(9), e15719.
- SONI, V., XIA, C., CHENG, C. K., NGUYEN, V. H., NGUYEN, D. L. T., BAJPAI, A., ... & RAIZADA, P. (2021). *Applied Materials Today*, 24, 101074.
- TU, S., GUO, Y., ZHANG, Y., HU, C., ZHANG, T., MA, T., & HUANG, H. (2020). *Advanced Functional Materials*, 30(48), 2005158.
- AKRAM, R., KHAN, M. D., ZEQUINE, C., ZHAO, C., GUPTA, R. K., AKHTAR, M. & BHATTI, M. H. (2020). *Materials science in semiconductor processing*, 109, 104925.
- UBANI, C. A., & IBRAHIM, M. A. (2019). *Materials Today: Proceedings*, 7, 646-654.
- ABDELWAHAB, A., CARRASCO-MARIN, F., & PÉREZ-CADENAS, A. F. (2020). *Materials*, 13(16), 3531.
- SAADI, H., KHALDI, O., PINA, J., COSTA, T., SEIXAS DE MELO, J. S., VILARINHO, P., & BENZARTI, Z. (2024). *Nanomaterials*, 14(1), 122.
- IBHADON, A. O., & FITZPATRICK, P. (2013). *Catalysts*, 3(1), 189-218.

ACKNOWLEDGEMENTS

The authors would like to thank the Coordenação de Aperfeiçoamento de Pessoal de Nível Superior (CAPES) - Financing Code 001, and the São Paulo Research Foundation (FAPESP) - Process n° 2022/04058-2, Process n° 2023/13127-0 and University of São Paulo (PUB USP Scholarships), for the financial support.